Progress in Chemical and Biochemical Research

Journal homepage: www.pcbiochemres.com

Original Research Article

Evaluation of Hot Corrosion of Hot Dip Aluminized Coated Superalloy IN738LC in Melted Na_2SO_4-25wt% NaCl Salt

Mohammad Sajjadnejad[1,*], Vahid Tavakoli Targhi[2], Seyyed Mohammad Saleh Haghshenas[3]

[1] *Department of Materials Engineering, School of Engineering, Yasouj University, Yasouj, Iran*
[2] *Department of Materials and Metallurgical Engineering, Amirkabir University of Technology (Tehran Polytechnic), Tehran, Iran*
[3] *Department of Materials Science and Engineering, School of Engineering, Shiraz University, Shiraz, Iran*

ARTICLEINFO

ARTICLE HISTORY

Submitted: 2023-12-24
Revised: 2024-01-16
Accepted: 2024-03-01
Available Online: 2024-04-18
ID: PCBR-2312-1331
Checked for Plagiarism: Yes
Language Editor Checked: Yes

KEYWORDS

Nickel-Based Superalloy
IN738LC
Hot-Dip Coating
Hot Corrosion
Aluminizing
Molten Salt

ABSTRACT

Superalloy IN738LC is categorized as one of the most frequently utilized nickel base superalloys in the production of hot section components due to its multiphase microstructure maximizing its strength under elevated temperatures. In this study, a hot dip diffusion coating of aluminum was employed on the nickel-base superalloy Inconel 738LC substrate to enhance the hot corrosion resistance required for high-temperature applications, such as turbine blades. The aluminizing salt bath included Al powder with a particular composition, NaCl, KCl, Na_3AlF_6, and NaF. A thickness of about 48 µm was attained by applying the coating for 30 minutes at 720 °C. Bare and aluminized coated specimens were subjected to hot corrosion assessment in molten salt, with a composition of Na_2SO_4-25wt% NaCl at 720 °C being exposed for 60 and 140 hours. Scanning electron microscopy (SEM), energy dispersive spectroscopy (EDS), and X-ray diffraction (XRD) were conducted on the coating sample to ensure the successful deposition of the hot dip aluminized layer. The aluminized sample exhibited excellent corrosion resistance owing to the formation of an Al_2O_3 layer, which meant that after 140 hours of testing; very little coating deterioration was detected. In contrast, the naked sample suffered severe degradation and showed poor hot corrosion resistance. It was thought that the aluminized sample's superior hot corrosion resistance resulted from the uniform and dense growth of an Al_2O_3 protective scale without any cracks on the superalloy surface

Citation: Mohammad Sajjadnejad, Vahid Tavakoli Targhi, Seyyed Mohammad Saleh Haghshenas. Evaluation of Hot Corrosion of Hot Dip Aluminized Coated Superalloy IN738LC in Melted Na_2SO_4-25wt%NaCl Salt. Prog. Chem. Biochem. Res., 7(2) (2024) 182-197
https://doi.org/10.48309/PCBR.2024.432210.1331
https://www.pcbiochemres.com/article_194320.html

* Corresponding author: Mohammad Sajjadnejad
✉ E-mail: m.sajjadnejad@yahoo.com; m.sajjadnejad@yu.ac.ir
☏ Tel number: +989378730497

GRAPHICAL ABSTRACT

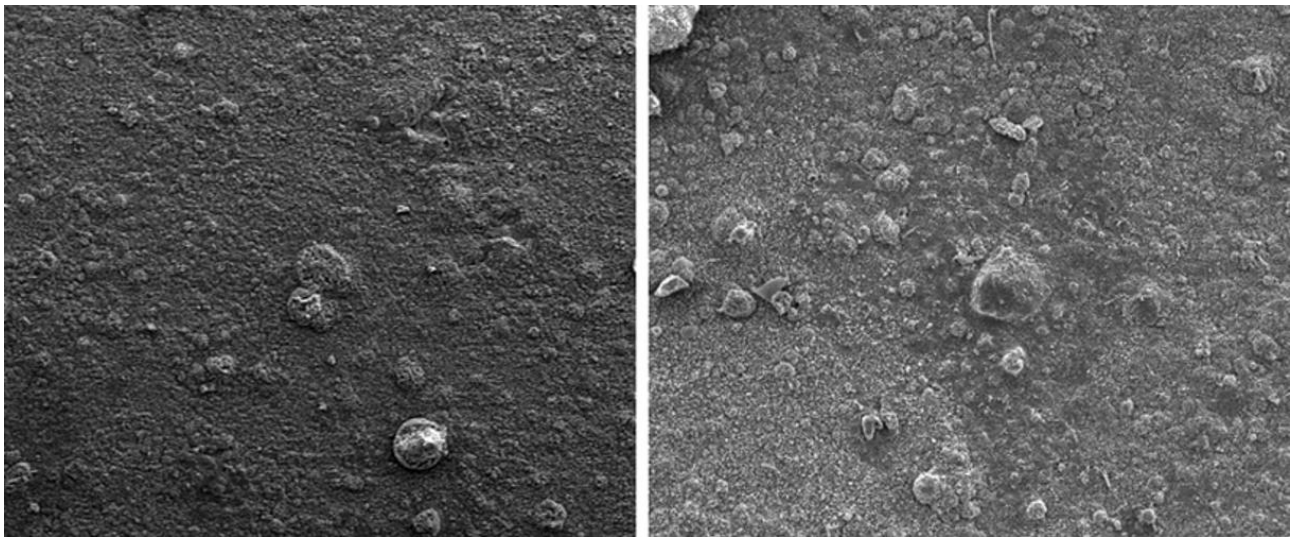

Introduction

In recent decades, nickel and nickel-based superalloys have been extensively applied in critical multi-areas including aviation, space, chemical and petrochemical industries [1-4]. Because of their notable high strength at high temperatures, significant resistance to oxidation and corrosion, high creep strength, heat resistance, excellent processability, and remarkable weldability, nickel-based superalloys are well-known as a class of high-performance alloys [5-7]. Nickel-based superalloys have introduced themselves as the enhancer of the life and efficiency of turbine engines under harsh conditions imposed by the turbine environment. They are thus widely used in gas turbine blades and other parts because of their superior high-temperature mechanical qualities [8-12], and above all these segments must demonstrate a high level of oxidation and corrosion resistance under the combustion environment conditions [13-15]. To be more specific, thermochemical surface treatments have been broadly applied to provide oxidation resistance [16]. Superalloy IN738LC is one of the most frequently utilized nickel base superalloys in the production of hot section components [4,17-19]. IN738LC is well-recognized for its multiphase microstructure, which enhances its strength at

high temperatures. This is achieved by the presence of small particles of the Ll_2 type ordered γ' [Ni_3(Al,Ti)] phase, which precipitate coherently inside the (FCC) γ matrix [20]. Surface coatings are broadly employed for these gamma prime materials, as the alloying requirements leads to a reduction in corrosion resistance. The primary concept of this technology involves choosing a substrate alloy with high strength to endure stress and applying a surface coating to provide optimal protection against corrosion from the environment [13]. Numerous techniques have been employed to fabricate a protective coating on Ni-based superalloys such as laser surface modification [21,22], high velocity oxy-fuel (HVOF) [23], ion implantation [24], electro-discharge coating [25,26], plasma spraying APS, LPPS, VPS, AXPS [27], and pack cementation [28]. The hot dip coating procedure is favorable among many surface modification methods due to its simplicity, speed, and cost-effectiveness [29]. Hot corrosion is a significant cause of failure in high temperature components

of essential technical systems, including aviation and engine-power turbines [30]. Several varieties of protective coatings have been shown to provide exceptional resistance to high temperature oxidation and hot corrosion [31-34]. Diffusion aluminide coatings are often used to effectively preserve jet engine components [35]. The development of an adhering layer of Al_2O_3 in diffusion aluminide coatings is a viable way for providing protection to super-alloys against corrosion. This method is widely utilized and highly desired [36-42]. An Al_2O_3 protective layer is well recognized for its superior oxidation resistance compared to other layers like Cr_2O_3. In addition, it remains intact without flaking even at high temperatures approaching 1300 °C. Furthermore, Al_2O_3 is very likely to provide sufficient resistance to oxidation for nickel-base superalloys [43-45] and it serves as a diffusion barrier that shields the substrate from fast deterioration [46]. Several methods are being employed to fabricate such an aluminide layer including electroplating, thermal spray coatings, chemical vapor deposition (CVD), pack aluminizing, laser cladding [47], electron-beam powder bed fusion [48], Reactive air aluminizing (RAA) [49], and hot dip coating [16]. According to the results of the study done by Barwinska *et al.* [50], hardness, fatigue response, service life, and high-temperature corrosion resistance of Inconel 740 nickel alloy were significantly improved by aluminizing through the chemical vapor deposition (CVD) process. This involved the use of $AlCl_3$ vapors, a hydrogen protective atmosphere, the temperature of 1040 °C, 8 hours, and an internal pressure of 150 hPa. Mottaghi Golshan *et al.* [51] examined the laser process parameters, including laser power, laser scanning speed, and powder feeding rate, to determine their impact on the geometrical characteristics of aluminized Inconel 738 superalloy produced through laser cladding. The findings of this study could serve as a valuable reference for aluminizing In738 using laser cladding technology. The cementation pack aluminizing process is often used to enhance the oxidation resistance of turbine blades made from Ni-based superalloys. The formation of a continuous, adherent, and slow-growing layer of α-Al_2O_3 is considered as crucial and very effective in achieving significant corrosion resistance for aluminide coatings. Aluminizing the surface of a nickel-based superalloy is a well-established and successful technique for creating and maintaining a protective Al_2O_3 scale [52]. The β-NiAl aluminide coating is susceptible to brittleness and sulfur-induced separation, mostly caused by grain boundary corrosion. This separation ultimately weakens the oxide-metal interface, leading to exfoliation [53]. Among the various techniques mentioned, Hot Dip Aluminizing (HDA) [54-58], is a diffusion coating method often used to provide high temperature oxidation- and corrosion-resistant coatings on stainless steels and low-alloy steels. The first use of the hot dip method for aluminizing Ni-base turbine blades occurred in 1952 [59]. The distinguished privileges of this technique are remarkable yield, low operating costs and significant applicability for large-size work-pieces [43,60] making hot-dip aluminizing a suitable technique [61,62], to develop a thick and adherent oxide layer of Al_2O_3 on the surface of aluminized components when they are subjected to an oxidizing environment [63-65] regulating the external infiltration of the alloying elements, while impeding the internal infiltration of corrosive substances [52].

Surveying the literature brings us about remarkable findings conducted on hot dip aluminizing alone and also modified aluminide coating type for hot corrosion resistance enhancement of Ni-based superalloys [66]. Accordingly, there have been scarce studies conducted on utilization of hot-dip aluminizing process through a solution containing Al powder and KCl/NaCl/NaF/Na_3AlF_6 molten salt. Thus, in this work, a novel hot-dip aluminizing process

has been employed to deposit aluminide coating on Ni-base superalloy Inconel 738. Finally, further characterizations including XRD, SEM and EDS are performed to investigate the hot corrosion behavior of the obtained specimens.

Experimental

Materials and specimens

A commercial, nickel-base superalloy, IN738LC, (15.96% Cr–1.63% Mo– 3.31% Ti–3.52% Al–0.69% Nb–1.83% Ta–3.08% W–8.53% Co–0.12% C, and Ni balance in wt.%), plate was used as the substrate material. Four specimens in the shape of a rectangle were cut to dimensions of 10×10×3 mm through a water-cooled cutting machine for corrosion tests. Before hot dip aluminizing, the specimens were degreased in an acetone bath subsequently cleaned by ultrasonic in an ethanol bath, and dried in air. The mixture of 12.0% aluminum powder and 88% salt (25.0% KCl–25.0% NaCl–28.0% Na_3AlF_6–10% NaF, in wt.%) was mixed and homogenized using a ball mill for 15 minutes. The mixture then was melted in an alumina crucible at 720 °C. Two of the specimens were hung by stainless steel wires and inserted into the crucible containing molten salt. After 30 min of insertion, the specimens were pulled out and air-cooled to room temperature. A mixed aqueous solution of nitric acid, phosphoric acid, and water in a 1:1:1 volume ratio at 25 °C was utilized to clean the hot-dipped specimen.

Hot corrosion tests

A supersaturated aqueous solution was prepared by mixing a corrosive medium consisting of a salt combination of Na_2SO_4-25%wt NaCl (in a ratio of 3:1) with distilled water. To achieve optimal adherence of the salt to the specimens, the samples were first subjected to a temperature of about 200 °C in an oven. Subsequently, the warm specimens were immersed in a supersaturated solution, resulting in the homogeneous deposition of a blended salt coating. The salt concentration on the surface of the samples was maintained at an average of 3 mg/cm^2. The specimens were positioned and dehydrated in a furnace, thereafter subjected to a temperature of about 720 °C, and maintained for durations of 60 and 140 hours. The specimens were extracted from the furnace and, at intervals of 20 hours, their weight was measured and they were subjected to salt exposure and subsequent testing. During the last step, the objects were immersed in hot water to separate any remaining salts. Weight measurements were conducted to assess the rate of hot corrosion. Table 1 indicates the samples coding.

Table1. Coding of the samples used in this study

Sample	Corrosion time	Coating
A60	60 h	Aluminized
A140	140 h	Aluminized
B60	60 h	Bare
B140	140 h	Bare

Characterization methods

X-ray diffraction (XRD) using EQUIPOX3000 model (INEL Co. France) with Cu-K_α radiation (λ = 1.540510 Å) radiation was employed in order to identify the phase structures of the specimen surface. The X-ray diffraction (XRD) instrument tube operated at a voltage of 40 kilovolts (kV) and an electric current of 30 milliamperes (mA). The specimens were analyzed by using scanning electron microscopy (SEM) in conjunction with energy-dispersive spectrometry (EDS) to analyze their cross-sections and surface morphologies. The coating's thickness was determined by analyzing microscopic inspection and EDS data, which included graphing the concentrations of elements against the depth from the surface.

Results and discussion

XRD characterization

Figure 1 depicts the XRD patterns of the IN738LC alloy in its original state (bare) and after exposure to hot corrosion at a temperature of 720 °C for 60 hours (B60) and 140 hours (B140). Based on the acquired X-ray patterns, it is

evident that the surface of the B60 sample shows the presence of Cr_2O_3, TiO_2, and $NiCr_2O_4$ phases after 60 hours of corrosion. While Cr_2O_3 exhibits a high level of corrosion resistance, TiO_2 and $NiCr_2O_4$ show a relatively low level of resistance to corrosion [41].

However, the XRD spectra of the B140 sample do not even exhibit any peaks corresponding to the Cr_2O_3 phase. To be more specified, the existence of Cr_2O_3 peaks in the XRD pattern of the coating sample exposed to the corrosive molten salt for 60 h is not necessarily sufficient for withstanding the corrosion attack due to the appearance of TiO_2 and $NiCr_2O_4$ compounds possessing low levels of corrosion resistance, and this shaky corrosion resistance was worsened by exposing for 140 hours as a result of disappearance of Cr_2O_3 peaks. Consequently, bare IN738LC lacks the ability to withstand hot corrosion conditions.

Figure 2 shows the XRD patterns of the aluminized coated samples before and after hot corrosion at 720 °C for 60 (A60) and 140 hours (A140). The existing peaks for aluminized coating before the corrosion test, at 32, 45, 55, and 67 °C correspond to (100), (110), (111), and (200) planes, respectively, which is attributed to NiAl phase. The obtained XRD pattern is in good consistency with the obtained XRD spectrum of NiAl phase in Aghayar's research [67].

According to Figure 2, XRD patterns of the A60 specimen confirm the existence of Al_2O_3 and NiAl diffraction peaks on the surface of the sample. The existence of Al_2O_3 leads to good corrosion resistance. Likewise, there was no trace of any other phases representing the destruction of the oxide layer. Furthermore, the X-ray pattern of the A140 specimen shows the presence of the $NiAl_2O_4$ phase, that reflects a very mild destruction in the surface [68].

Microstructure analysis

Figure 3 clearly illustrates the cross-sectional BSE images of the aluminized coating prior to the hot corrosion investigation. A diffusion coating, about 48 ± 0.2 µm thick, is present between the aluminum layer and the substrate. This is shown by the vertical green line in the illustration.

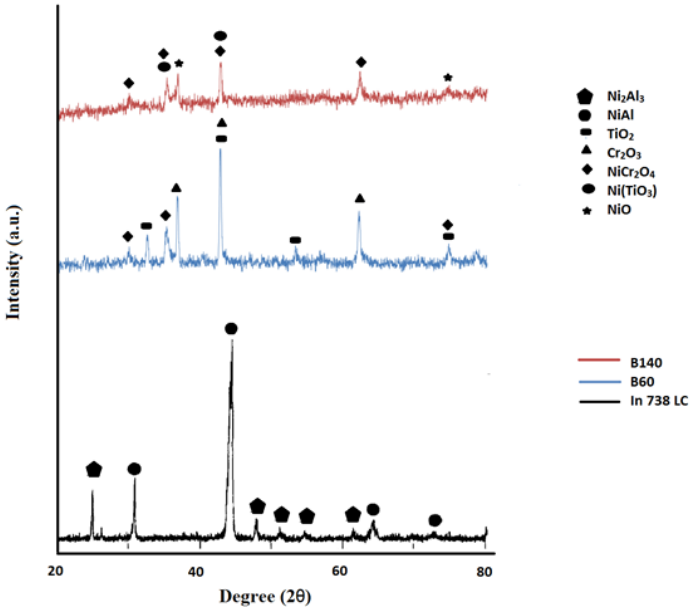

Fig 1.XRD patterns of the bare IN738LC before and after corrosion at 720 °C for 60 and 140 hours in the salt of Na_2SO_4-25wt% NaCl

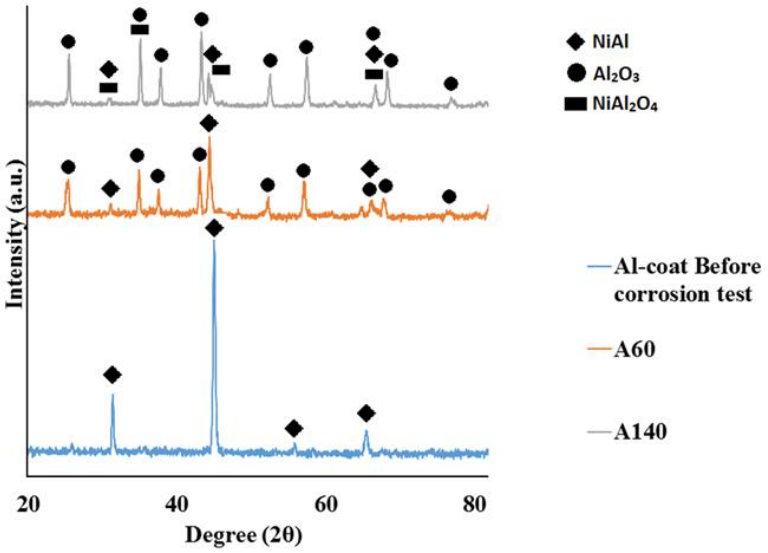

Fig 2.XRD patterns of the aluminized coating before and after corrosion at 720 °C for 60 and 140 hours in the salt of Na_2SO_4-25wt% NaCl

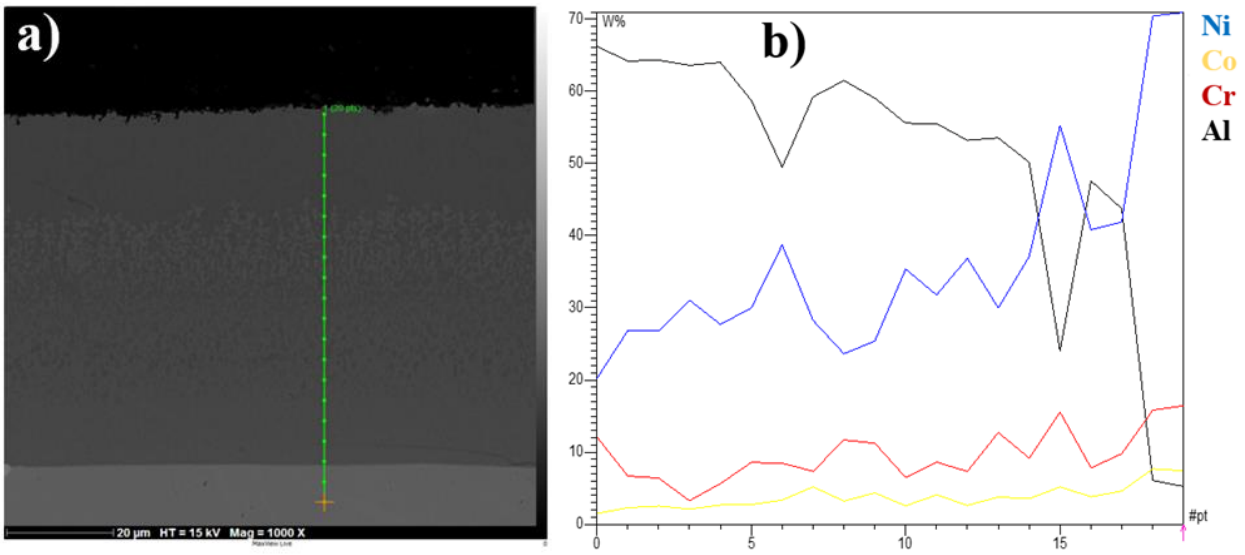

Fig 3. Cross-sectional BSE images of the aluminized coating specimens with a thickness of about 48 µm before the corrosion test

The coating consists of both exterior and interior zones. The interior region has a compact and homogeneous composition, while the surrounding region displays a porous composition. The figure demonstrates that the coating possesses a continuous and solid structure, with the major parts equally distributed and no visible fractures. In addition, the coating displays strong adherence to the substrate. Figure 3 shows the diffusion curve over the coatings' thickness, indicating the outward diffusion of the substrate components. Spots 1-4, 5-17, and 18-20 corresponded to the aluminum topcoat, diffusion layer, and the IN738LC superalloy substrate, respectively. Table 2 displays the allocation and proportion of various constituents in the coating. There is 66% Al and 20% Ni in the exterior layer of the coating,

while in the coating-substrate interface, 44% Al and 42% Ni were found. X-ray diffraction of the coated specimen showed that the coating was composed mainly of one phase which was NiAl. Hence, this is in good agreement with the EDS results and Ni-Al phase diagram [69], which showed the downward diffusion of Al.

The NiAl synthesis on the substrate in hot-dip aluminize coating in the molten salt is facilitated by the generation of Al3+ ions in a mixture of molten chloride alkali metals, Al powder, and Na_3AlF_6 in which the reaction (1) would be written as below [70]:

$$2Al^0 + Al^{3+} = 3Al^+ \quad (1)$$

The obtained Al^+ ions can react with elements possessing higher levels of electronegativity. Since the substrate used in this study is a Ni-based superalloy, the NiAl phase could be obtained as a result of the reaction (2):

$$3Al^+ + 2Ni = 2NiAl + Al^{3+} \quad (2)$$

Figure 4a demonstrates the cross-sectional BSE image of the bare IN738LC before the hot corrosion test. According to the EDS results (Fig 4b), the white-colored deposit in the coating (point A) is mainly composed of Ti, Ta, and W. This also implies that the Al elements had diffused into the substrate.

Table2. Distribution and the relative content of various elements in the coating

Distance from surface coating (µm)	Ni content (%)	Al content (%)	Cr content (%)	Co content (%)
0	20	66	12	1.5
10	27	64	5.6	2.6
20	39	49	8.5	3
30	37	53	7	2
40	41	47	8	4
47	42	44	9	5

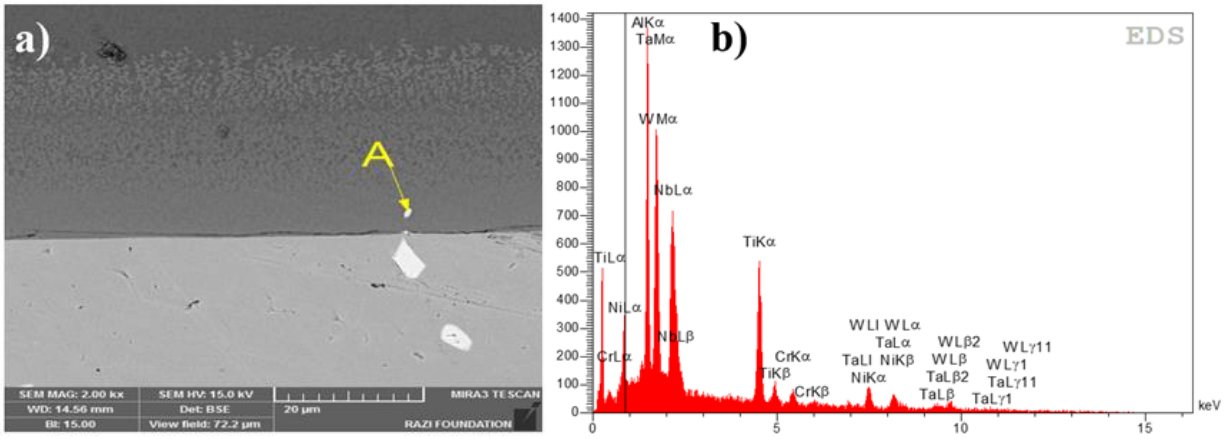

Fig 4.SEM images (a) and EDS analysis of A point (b) in bare IN738LC before the hot corrosion test

Hot corrosion behavior

Figure 5 displays the cross-sectional view of the A60 and A140 specimens. The coating and the interface between the coating and substrate remain intact, with no visible cracks even in the A140 sample. This indicates that the coating effectively protects IN738LC against hot corrosion. In addition, after 140 hours of heat corrosion, the microstructure of the layers and coating surface became flattened. The EDS findings further indicate that the substrate components are well-shielded from hot corrosion due to the existence of a protective layer composed of Al_2O_3.

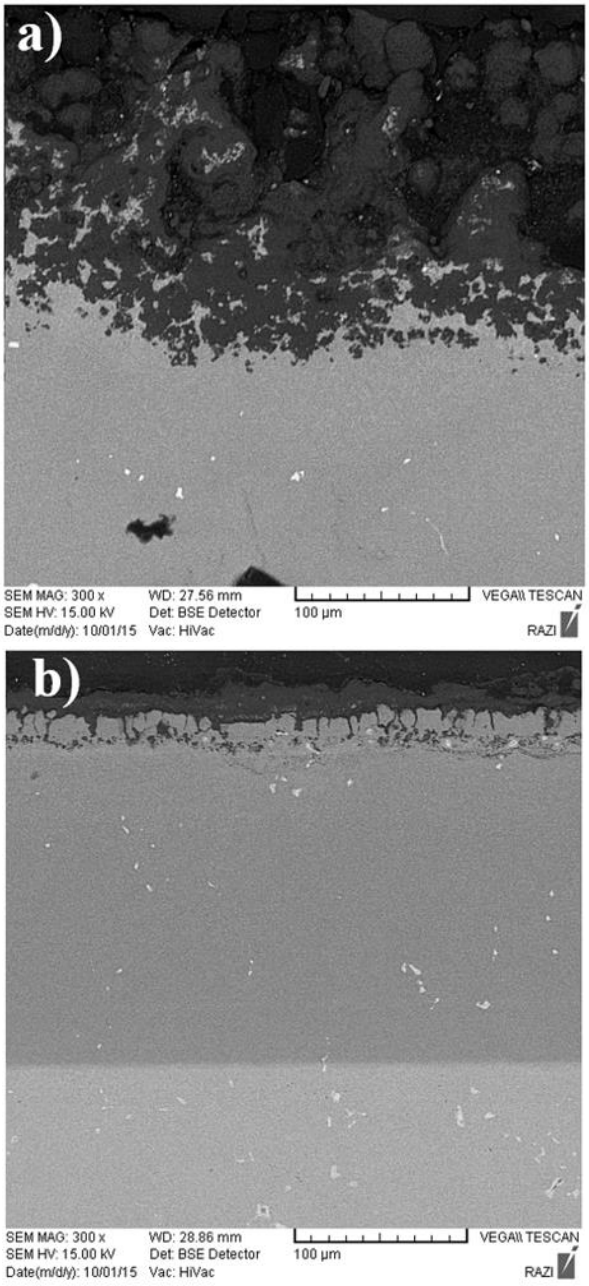

Fig 5. Line scanning images on the cross-sections of the aluminized coating specimen after corrosion at 720 °C for (a) 60 and (b) 140 hours in the salt of Na_2SO_4-25wt% NaCl

Figure 6 depicts the cross-sectional view of the B60 and B140 specimens. Upon observing the sample surface after 60 hours of heat corrosion, it is evident that corrosion has occurred and the resulting corrosion product has suffered some minor damage.

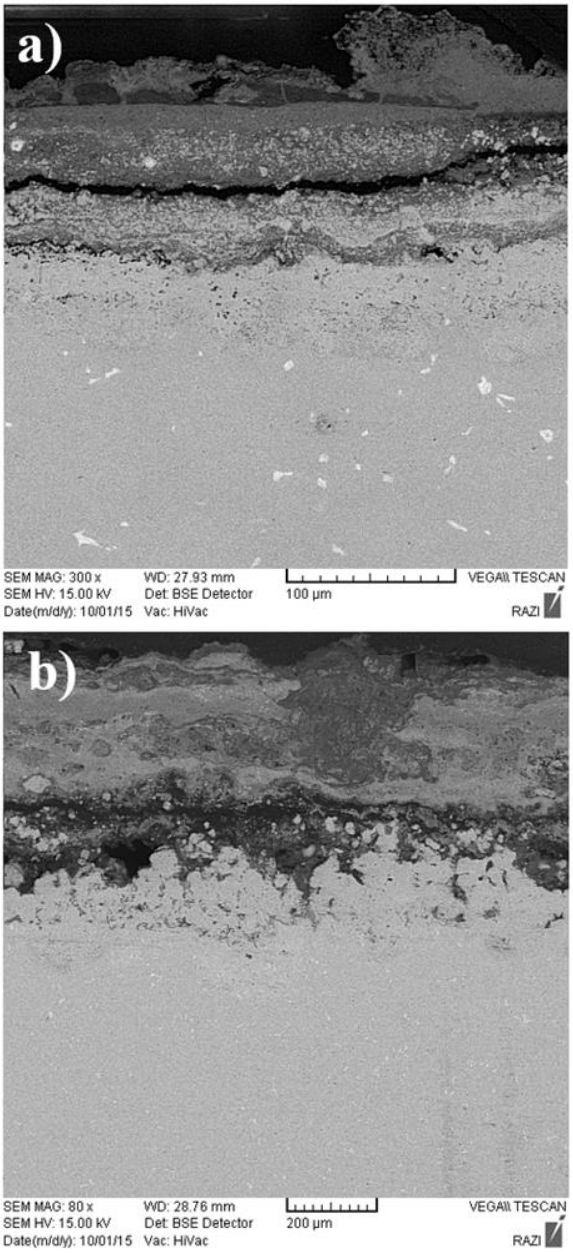

Fig 6. Cross-section of the hot corroded uncoated sample after corrosion at 720 °C for (a) 60 and (b) 140 hours in the salt of Na_2SO_4-25wt% NaCl

Furthermore, when the corrosion period increases, the spread of corrosive components and the depth of corrosion diffusion progressively increase. The corrosion process involves the gradual production of layers of reaction products along the contact, resulting in the creation of a laminar structure. These layers exhibit rapid growth and are readily separated

from the surface. Moreover, the Energy Dispersive Spectroscopy (EDS) analysis of this sample reveals that essential components like Nickel (Ni) and Chromium (Cr) from the substrate are involved in the corrosion processes. The damage process is similar to thermal oxidation, but the presence of corrosive salts in molten form intensifies the damage, leading to the development of corrosion phenomena. This intensified corrosion damage is clearly seen at the grain boundaries. Figure 7a and 7b show the SEM images of the A60 and A140 specimens. Obviously, the Al_2O_3 layer is formed after 60 hours which is consistent with the XRD analysis. By increasing the corrosion time to 140 h, no particular change was observed in the morphology; however, the oxide layer is marginally scaled.

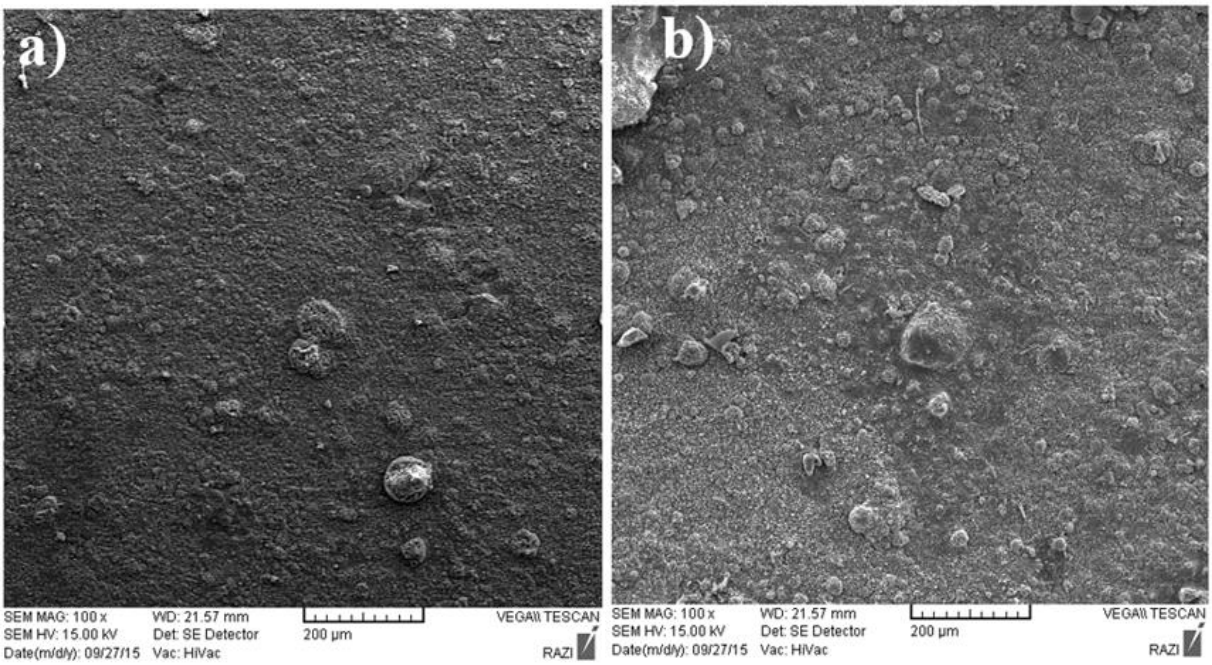

Fig 7.SEM images of the hot-dip aluminized sample after hot corrosion test for (a) 60 and (b) 140 hours

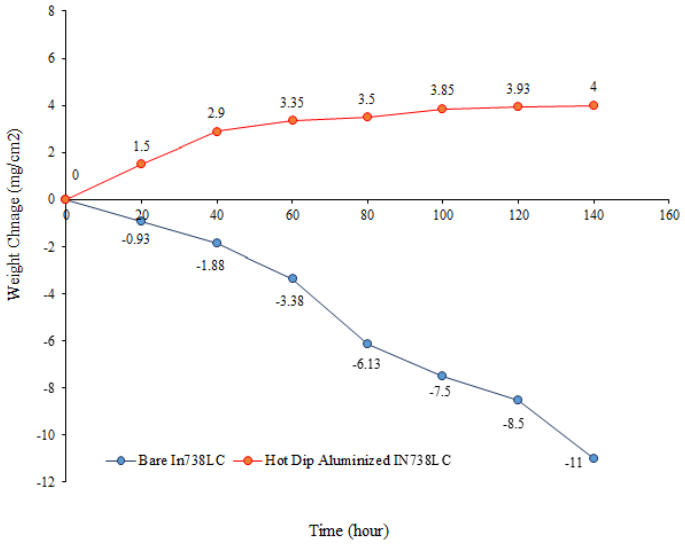

Fig 8. Weight change of hot corrosion test for coated and bare specimens

Corrosion kinetics

The hot corrosion kinetic figures of the bare and the aluminized coated IN738LC are illustrated in Figure 8.

The mass change involves an increase in mass (reaching a weight limit of 4 mg/cm^2 after 120 hours) due to the development of scales, and a decrease in mass (with a progressively steeper slope) caused by the shedding of scales. Therefore, the change in mass of the specimen in molten salt reflects the combined influence of these two processes.

The uncoated and the aluminized coated IN738LC alloy exhibit distinct corrosion characteristics when exposed to molten salt. According to the information shown in Figure 8, the IN738LC material exhibits poor resistance to heat corrosion, which may be related to the volatile nature of chloride. Due to the low melting temperatures and high vapor pressure of most metal chlorides, chlorine has a tendency to rapidly diffuse out through the oxide scale. It then reacts with alloying elements such as aluminum and chromium at the oxide/metal interface, resulting in the formation of volatile chlorides [41,71]. Moreover, the Cr_2O_3 creation might contribute to weight reduction due to the evaporation of chromium oxides and hydroxides, resulting in the loss of Cr from the surface. Moreover, the significant decrease in the curve might be attributed to the existence of low-melting-point phases located at the interfaces between grains, which serve as efficient pathways for diffusion [13]. The molten salt may quickly disperse and react with the alloy via these pathways. The use of an aluminized coating enhanced the alloy's resistance to heat corrosion. The first stage of exposure to the molten salt combination resulted in a significant rise in mass, reaching a maximum gain of 2.9 mg/cm^2 after about 40 hours. Subsequently, the mass gain stabilized at a relatively low level, indicating a stable state in the second stage. It may be inferred that during the second stage, the rate at which the oxidation film grew was equal to the rate at which it peeled off.

Conclusion

An aluminized coating was applied to the Ni-based superalloy IN738LC by immersing it in a combination of Al powder and molten salt consisting of KCl, NaCl, NaF, and Na_3AlF_6. The molten salt facilitates the formation of a dense and homogeneous coating with a high concentration of aluminum. The data obtained show that the coating consists mostly of a NiAl matrix. Subsequent experiments revealed that the uncoated Ni-based superalloy IN738LC had a low resistance to corrosion in high-temperature corrosive conditions, while the aluminized coating, with a thickness of about 48 µm, exhibited exceptional resistance to corrosion in the Na_2SO_4-25wt% NaCl salt combination at 720 °C. This resistance may be attributed to the creation of the Al_2O_3 phase.

ORCID

Mohammad Sajjadnejad
https://orcid.org/0000-0001-5112-1791
Vahid Tavakoli Targhi
https://orcid.org/0000-0002-3934-4682
Seyyed Mohammad Saleh Haghshenas
https://orcid.org/0000-0001-5878-8214

Funding

The authors declare that no funds, grants, or other support were received during the preparation of this manuscript.

Declarations

Conflict of interest: The authors have no relevant financial or non-financial interests to disclose.
Ethical approval: Not applicable.
Consent to participate: Not applicable.
Consent for publication: Not applicable

References

1. de Vasconcelos Varela A, de Deus HD, de Siqueira MC, Rezende MC, de Almeida LH.

Oxidation assisted intergranular cracking in 718 Nickel Superalloy: on the mechanism of dynamic embrittlement. Journal of Materials Research and Technology. 2018 Jul 1;7(3):319-25. [Crossref], [Google Scholar], [Publisher]
2. Zhang F, Levine LE, Allen AJ, Stoudt MR, Lindwall G, Lass EA, Williams ME, Idell Y, Campbell CE. Effect of heat treatment on the microstructural evolution of a nickel-based superalloy additive-manufactured by laser powder bed fusion. Acta materialia. 2018 Jun 15;152:200-14. [Crossref], [Google Scholar], [Publisher]
3. Ekrami M, Shahbazi Karami J, Araee A, Sharifianjazi F, Sadeghi E, Moghanian A. Fabrication of copper/stainless steel bimetallic couple, by diffusion bonding using silver and nickel foils as interlayers. Inorganic and Nano-Metal Chemistry. 2019 May 4;49(5):152-62. [Crossref], [Google Scholar], [Publisher]
4. Targhi VT, Omidvar H, Hadavi SM, Sharifianjazi F. Microstructure and hot corrosion behavior of hot dip siliconized coating on Ni-base superalloy IN738LC. Materials Research Express. 2020 May 29;7(5):056527. [Crossref], [Google Scholar], [Publisher]
5. Cieślik I, Duchna M, Płociński T, Wyszkowska E, Azarov A, Zieniuk M. Ion irradiation effect on the microstructure of Inconel 625 obtained by Selective Laser Melting and by the metallurgical process. Surface and Coatings Technology. 2020 Aug 25;396:125952. [Crossref], [Google Scholar], [Publisher]
6. Shankar V, Rao KB, Mannan SL. Microstructure and mechanical properties of Inconel 625 superalloy. Journal of nuclear materials. 2001 Feb 1;288(2-3):222-32. [Crossref], [Google Scholar], [Publisher]
7. Gajalappa Y, Krishnaiah A, Kumar KB, Saxena KK, Goyal P. Flow behaviour kinetics of Inconel 600 superalloy under hot deformation using gleeble 3800. Materials Today: Proceedings. 2021 Jan 1;45:5320-2. [Crossref], [Google Scholar], [Publisher]
8. Y. Aoki, A. Sato, Method of making a Ni—based single crystal superalloy and turbine blade incorporating same, Google Patents, 2018. [Crossref], [Google Scholar], [Publisher]
9. Rezaei M, Kermanpur A, Sadeghi F. Effects of withdrawal rate and starter block size on crystal orientation of a single crystal Ni-based superalloy. Journal of crystal growth. 2018 Mar 1;485:19-27. [Crossref], [Google Scholar], [Publisher]
10. Montero X, Ishida A, Meißner TM, Murakami H, Galetz MC. Effect of surface treatment and crystal orientation on hot corrosion of a Ni-based single-crystal superalloy. Corrosion Science. 2020 Apr 15;166:108472. [Crossref], [Google Scholar], [Publisher]
11. Tang Z, Dong X, Geng Y, Wang K, Duan W, Gao M, Mei X. The effect of warm laser shock peening on the thermal stability of compressive residual stress and the hot corrosion resistance of Ni-based single-crystal superalloy. Optics & Laser Technology. 2022 Feb 1;146:107556. [Crossref], [Google Scholar], [Publisher]
12. Yang YQ, Zhao YC, Wen ZX, Lu GX, Pei HQ, Yue ZF. Synergistic effect of multiple molten salts on hot corrosion behaviour of Ni-based single crystal superalloy. Corrosion Science. 2022 Aug 1;204:110381. [Crossref], [Google Scholar], [Publisher]
13. Wu D, Jiang S, Fan Q, Gong J, Sun C. Hot corrosion behavior of a Cr-modified aluminide coating on a Ni-based superalloy. Acta Metallurgica Sinica (English Letters). 2014 Aug;27:627-34. [Crossref], [Google Scholar], [Publisher]

14. Lv P, Sun X, Cai J, Zhang C, Liu X, Guan Q. Microstructure and high temperature oxidation resistance of nickel based alloy GH4169 irradiated by high current pulsed electron beam. Surface and Coatings Technology. 2017 Jan 15;309:401-9. [Crossref], [Google Scholar], [Publisher]
15. Ramkumar KD, Abraham WS, Viyash V, Arivazhagan N, Rabel AM. Investigations on the microstructure, tensile strength and high temperature corrosion behaviour of Inconel 625 and Inconel 718 dissimilar joints. Journal of Manufacturing Processes. 2017 Jan 1;25:306-22. [Crossref], [Google Scholar], [Publisher]
16. Yener T, Doleker KM, Erdogan A, Oge M, Er Y, Karaoglanli AC, Zeytin S. Wear and oxidation performances of low temperature aluminized IN600. Surface and Coatings Technology. 2022 Apr 25;436:128295. [Crossref], [Google Scholar], [Publisher]
17. Rani S, Agrawal AK, Rastogi V. Failure analysis of a first stage IN738 gas turbine blade tip cracking in a thermal power plant. Case studies in engineering failure analysis. 2017 Apr 1;8:1-0. [Crossref], [Google Scholar], [Publisher]
18. Mallikarjuna HT, Caley WF, Richards NL. Oxidation kinetics and oxide scale characterization of nickel-based superalloy IN738LC at 900° C. Journal of Materials Engineering and Performance. 2017 Oct;26:4838-46. [Crossref], [Google Scholar], [Publisher]
19. Messé OM, Muñoz-Moreno R, Illston T, Baker S, Stone HJ. Metastable carbides and their impact on recrystallisation in IN738LC processed by selective laser melting. Additive Manufacturing. 2018 Aug 1;22:394-404. [Crossref], [Google Scholar], [Publisher]
20. Kolagar AM, Tabrizi N, Cheraghzadeh M, Shahriari MS. Failure analysis of gas turbine first stage blade made of nickel-based superalloy. Case studies in engineering failure analysis. 2017 Apr 1;8:61-8. [Crossref], [Google Scholar], [Publisher]
21. Dai J, Zhang F, Wang A, Yu H, Chen C. Microstructure and properties of Ti-Al coating and Ti-Al-Si system coatings on Ti-6Al-4V fabricated by laser surface alloying. Surface and Coatings Technology. 2017 Jan 15;309:805-13. [Crossref], [Google Scholar], [Publisher]
22. Wu Y, Wang AH, Zhang Z, Zheng RR, Xia HB, Wang YN. Laser alloying of Ti–Si compound coating on Ti–6Al–4V alloy for the improvement of bioactivity. Applied Surface Science. 2014 Jun 30;305:16-23. [Crossref], [Google Scholar], [Publisher]
23. Saeidi S, Voisey KT, McCartney DG. Mechanical properties and microstructure of VPS and HVOF CoNiCrAlY coatings. Journal of Thermal Spray Technology. 2011 Dec;20:1231-43. [Crossref], [Google Scholar], [Publisher]
24. Oliveira AC, Oliveira RD, Reis DA, Carreri FD. Effect of nitrogen high temperature plasma based ion implantation on the creep behavior of Ti-6Al-4V alloy. Applied Surface Science. 2014 Aug 30;311:239-44. [Crossref], [Google Scholar], [Publisher]
25. Tijo D, Masanta M. Mechanical performance of in-situ TiC-TiB2 composite coating deposited on Ti-6Al-4V alloy by powder suspension electro-discharge coating process. Surface and Coatings Technology. 2017 Nov 15;328:192-203. [Crossref], [Google Scholar], [Publisher]
26. Bazli M, Zhao XL, Bai Y, Raman RS, Al-Saadi S. Bond-slip behaviour between FRP tubes and seawater sea sand concrete. Engineering Structures. 2019

Oct 15;197:109421. [Crossref], [Google Scholar], [Publisher]
27. Kumari R, Majumdar JD. Studies on corrosion resistance and bio-activity of plasma spray deposited hydroxylapatite (HA) based TiO2 and ZrO2 dispersed composite coatings on titanium alloy (Ti-6Al-4V) and the same after post spray heat treatment. Applied Surface Science. 2017 Oct 31;420:935-43. [Crossref], [Google Scholar], [Publisher]
28. Afshar A, Sabour A, Saremi M, Ghasemi D. Improving high temperature oxidation and hot corrosion resistance of Ni-base super alloy INC738LC with Cr-Si-RE modified aluminide coatings produced by single step pack cementation process. Protection of Metals and Physical Chemistry of Surfaces. 2012 Jan;48:120-7. [Crossref], [Google Scholar], [Publisher]
29. Sadeq FO, Sharifitabar M, Afarani MS. Synthesis of Ti–Si–Al coatings on the surface of Ti–6Al–4V alloy via hot dip siliconizing route. Surface and Coatings Technology. 2018 Mar 15;337:349-56. [Crossref], [Google Scholar], [Publisher]
30. Shirvani K, Saremi M, Nishikata A, Tsuru T. Electrochemical study on hot corrosion of Si-modified aluminide coated In-738LC in Na2SO4–20 wt.% NaCl melt at 750° C. Corrosion Science. 2003 May 1;45(5):1011-21. [Crossref], [Google Scholar], [Publisher]
31. Anand K, Lau YC, Mathew P, Pabla SS, Sundararajan G, Nayak M, inventors; General Electric Co, assignee. Erosion and corrosion resistant coatings for exhaust gas recirculation based gas turbines. United States patent US 9,365,932. 2016 Jun 14. [Google Scholar], [Publisher]
32. Mahade S, Jonnalagadda KP, Curry N, Li XH, Björklund S, Markocsan N, Nylén P, Peng RL. Engineered architectures of gadolinium zirconate based thermal barrier coatings subjected to hot corrosion test. Surface and Coatings Technology. 2017 Nov 15;328:361-70. [Crossref], [Google Scholar], [Publisher]
33. Gurrappa I, Yashwanth IV, Mounika I, Murakami H, Kuroda S. The importance of hot corrosion and its effective prevention for enhanced efficiency of gas turbines. Gas Turbines-Materials, Modeling and Performance. 2015 Feb 25;1:55-102. [Crossref], [Google Scholar], [Publisher]
34. Mishra RK. Fouling and corrosion in an aero gas turbine compressor. Journal of Failure Analysis and Prevention. 2015 Dec;15(6):837-45. [Crossref], [Google Scholar], [Publisher]
35. Adamiak S, Bochnowski W, Dziedzic A, Filip R, Szeregij E. Structure and properties of the aluminide coatings on the Inconel 625 superalloy. High Temperature Materials and Processes. 2016 Jan 1;35(1):103-12. [Crossref], [Google Scholar], [Publisher]
36. Afshar A, Sabour A, Saremi M, Ghasemi D. Improving high temperature oxidation and hot corrosion resistance of Ni-base super alloy INC738LC with Cr-Si-RE modified aluminide coatings produced by single step pack cementation process. Protection of Metals and Physical Chemistry of Surfaces. 2012 Jan;48:120-7. [Crossref], [Google Scholar], [Publisher]
37. Masoudian A, Karbasi M, SharifianJazi F, Saidi A. Developing Al2O3-TiC in-situ nanocomposite by SHS and analyzingtheeffects of Al content and mechanical activation on microstructure. Journal of Ceramic Processing Research. 2013 Aug 1;14(4):486-91. [Google Scholar], [Publisher]
38. Jazi EH, Esalmi-Farsani R, Borhani G, Jazi FS. Synthesis and Characterization of In Situ Al-Al13Fe4-Al2O3-TiB2 Nanocomposite Powder by Mechanical Alloying and Subsequent Heat Treatment. Synthesis and Reactivity in Inorganic,

Metal-Organic, and Nano-Metal Chemistry. 2014 Feb 7;44(2):177-84. [Crossref], [Google Scholar], [Publisher]
39. Masoudian A, Tahaei A, Shakiba A, Sharifianjazi F, Mohandesi JA. Microstructure and mechanical properties of friction stir weld of dissimilar AZ31-O magnesium alloy to 6061-T6 aluminum alloy. Transactions of nonferrous metals society of China. 2014 May 1;24(5):1317-22. [Crossref], [Google Scholar], [Publisher]
40. Alizadeh M, Paydar MH, Jazi FS. Structural evaluation and mechanical properties of nanostructured Al/B4C composite fabricated by ARB process. Composites Part B: Engineering. 2013 Jan 1;44(1):339-43. [Crossref], [Google Scholar], [Publisher]
41. Shirvani K, Rashidghamat A. Evolution of oxide scale on aluminide and Pt-aluminide coatings exposed to type I (870 C) hot corrosion. Oxidation of Metals. 2016 Feb;85:75-85. [Crossref], [Google Scholar], [Publisher]
42. Bermejo Sanz J, Roussel García R, Kolarik V, Juez Lorenzo MD. Influence of the slurry thickness and heat treatment parameters on the formation of aluminium diffusion coating. Oxidation of Metals. 2017 Aug;88:179-90. [Crossref], [Google Scholar], [Publisher]
43. Wang CJ, Chen SM. Microstructure and cyclic oxidation behavior of hot dip aluminized coating on Ni-base superalloy Inconel 718. surface and Naumenko D, Jalowicka A, Nowak W, Quadakkers WJ. Corrosion resistance of cast, nickel base superalloys in environments relevant to gas-turbines operating on sulfur rich fuels. InNACE Corrosion 2016 Mar 6 (pp. NACE-2016). NACE. [Crossref], [Google Scholar], [Publisher]
44. Kraemer KM, Baumann C, Mueller F, Oechsner M. On the Corrosive Behaviour of Nickel-based superalloys for turbine engines: Oxide growth and internal microstructural degradation. InProceedings of the 123himat Conference 2015 (pp. 234-237). [Google Scholar].
45. Szkliniarz W, Moskal G, Szkliniarz A, Swadźba R. The Influence of Aluminizing Process on the Surface Condition and Oxidation Resistance of Ti–45Al–8Nb–0.5 (B, C) Alloy. Coatings. 2018 Mar 20;8(3):113. [Crossref], [Google Scholar], [Publisher]
46. Golshan BM, Ganjali M. Characteristics of the aluminized IN738 superalloy using laser cladding method. Lasers in Manufacturing and Materials Processing. 2023 Jun;10(2):312-29. [Crossref], [Google Scholar], [Publisher]
47. Luo M, Liao X, Ringer SP, Primig S, Haghdadi N. Grain boundary network evolution in electron-beam powder bed fusion nickel-based superalloy Inconel 738. Journal of Alloys and Compounds. 2024 Jan 25;972:172811. [Crossref], [Google Scholar], [Publisher]
48. Sarraf SH, Soltanieh M, Rastegari S. Reactive air aluminizing of a nickel-based superalloy (IN738LC): Coating formation mechanism. Surface and Coatings Technology. 2023 Mar 15;456:129229. [Crossref], [Google Scholar], [Publisher]
49. Barwinska I, Kopec M, Kukla D, Łazińska M, Sitek R, Kowalewski ZL. Effect of Aluminizing on the Fatigue and High-Temperature Corrosion Resistance of Inconel 740 Nickel Alloy. JOM. 2023 May;75(5):1482-94. [Crossref], [Google Scholar], [Publisher]
50. Mottaghi Golshan B, Hadavi MM, Ganjali M. Effects of Laser Process Parameters on Geometrical Characteristics of Aluminized Inconel738 superalloy by laser cladding. Journal of Physical & Theoretical Chemistry. 2021 Nov

1;18(2):45-54. [Crossref], [Google Scholar], [Publisher]
51. Koo CH, Bai CY, Luo YJ. The structure and high temperature corrosion behavior of pack aluminized coatings on superalloy IN-738LC. Materials chemistry and physics. 2004 Aug 1;86(2-3):258-68. [Crossref], [Google Scholar], [Publisher]
52. Ma J, Jiang SM, Li HQ, Wang WX, Gong J, Sun C. Microstructure and oxidation behaviour of an AlSiY/NiCrAlYSi composite coating at 1150 C. Corrosion science. 2011 Apr 1;53(4):1417-23. [Crossref], [Google Scholar], [Publisher]
53. Lemmens B, Springer H, De Graeve I, De Strycker J, Raabe D, Verbeken K. Effect of silicon on the microstructure and growth kinetics of intermetallic phases formed during hot-dip aluminizing of ferritic steel. Surface and Coatings Technology. 2017 Jun 15;319:104-9. [Crossref], [Google Scholar], [Publisher]
54. Hung JC, Ku CY, Ger MD, Fen ZW. Fabrication of an electrode insulation layer for electrochemical machining by using hot dip aluminizing and micro-arc oxidation method. Procedia Cirp. 2016 Jan 1;42:390-5. [Crossref], [Google Scholar], [Publisher]
55. Huilgol P, Udupa KR, Bhat KU. Metastable microstructures at the interface between AISI 321 steel and molten aluminum during hot-dip aluminizing. Surface and Coatings Technology. 2018 Aug 25;348:22-30. [Crossref], [Google Scholar], [Publisher]
56. Sah SP, Tada E, Nishikata A. Enhancing corrosion resistance of type 310S stainless steel in carbonate melt by hot-dip aluminizing. Journal of The Electrochemical Society. 2018 May 19;165(7):C403. [Crossref], [Google Scholar], [Publisher]
57. Zang J, Song P, Feng J, Xiong X, Chen R, Liu G, Lu J. Oxidation behaviour of the nickel-based superalloy DZ125 hot-dipped with Al coatings doped by Si. Corrosion Science. 2016 Nov 1;112:170-9. [Crossref], [Google Scholar], [Publisher]
58. Davis JR, editor. Surface engineering for corrosion and wear resistance. ASM international; 2001. [Google Scholar], [Publisher]
59. Tsaur CC, Rock JC, Chang YY. The effect of NaCl deposit and thermal cycle on an aluminide layer coated on 310 stainless steel. Materials chemistry and physics. 2005 Jun 15;91(2-3):330-7. [Crossref], [Google Scholar], [Publisher]
60. Patel P, Jamnapara NI, Zala A, Kahar SD. Investigation of hot-dip aluminized Ti6Al4V alloy processed by different thermal treatments in an oxidizing atmosphere. Surface and Coatings Technology. 2020 Mar 15;385:125323. [Crossref], [Google Scholar], [Publisher]
61. Targhi VT, Omidvar H, Sharifianjazi F, Pakseresht A. Hot corrosion behavior of aluminized and Si-modified aluminized coated IN-738LC produced by a novel hot-dip process. Surfaces and Interfaces. 2020 Dec 1;21:100599. [Crossref], [Google Scholar], [Publisher]
62. Ho CJ, Hsieh YJ, Rashidi S, Orooji Y, Yan WM. Thermal-hydraulic analysis for alumina/water nanofluid inside a mini-channel heat sink with latent heat cooling ceiling-An experimental study. International Communications in Heat and Mass Transfer. 2020 Mar 1;112:104477. [Crossref], [Google Scholar], [Publisher]
63. Hossein-Zadeh M, Ghasali E, Mirzaee O, Mohammadian-Semnani H, Alizadeh M, Orooji Y, Ebadzadeh T. An investigation into the microstructure and mechanical properties of V2AlC MAX phase prepared by microwave sintering. Journal of Alloys and Compounds. 2019 Jul 30;795:291-

303. [Crossref], [Google Scholar], [Publisher]
64. Zhang K, Jang HW, Van Le Q. Production methods of ceramic-reinforced Al-Li matrix composites: A review. Journal of Composites and Compounds. 2020 Jun 30;2(3):77-84. [Crossref], [Google Scholar], [Publisher]
65. Fan QX, Jiang SM, Yu HJ, Gong J, Sun C. Microstructure and hot corrosion behaviors of two Co modified aluminide coatings on a Ni-based superalloy at 700 C. Applied Surface Science. 2014 Aug 30;311:214-23. [Crossref], [Google Scholar], [Publisher]
66. Aghayar Y, Khorasanian M, Lotfi B. High temperature behavior of diffusion aluminide coating on alloy 600 superalloy. Materials at High Temperatures. 2018 Jul 4;35(4):343-54. [Crossref], [Google Scholar], [Publisher]
67. Firouzi A, Shirvani K. The structure and high temperature corrosion performance of medium-thickness aluminide coatings on nickel-based superalloy GTD-111. Corrosion science. 2010 Nov 1;52(11):3579-85. [Crossref], [Google Scholar], [Publisher]
68. [69] L. Kaufman, H. Nesor, Calculation of superalloy phase diagrams: Part II, Metallurgical Transactions 5(7) (1974) 1623-1629. [Crossref], [Google Scholar], [Publisher]
69. Ilyushchenko NG, Belyaeva GI. Low-temperature aluminizing of steels in molten salts. Metal Science and Heat Treatment. 1968 Apr;10(4):261-4. [Crossref], [Google Scholar], [Publisher]
70. Sidhu TS, Malik A, Prakash S, Agrawal RD. Cyclic oxidation behavior of Ni-and Fe-based superalloys in air and Na2SO4-25% NaCl molten salt environment at 800° C. International Journal of Physical Sciences. 2006 Sep 30;1(1):27-33. [Google Scholar], [Publisher].